

# Green Function Simulation of Hamiltonian Lattice Models with Stochastic Reconfiguration

Matteo Beccaria

*Dipartimento di Fisica dell'Università di Lecce, I-73100, Italy,  
Istituto Nazionale di Fisica Nucleare, Sezione di Lecce*

## Abstract

We apply a recently proposed Green Function Monte Carlo to the study of Hamiltonian lattice gauge theories. This class of algorithms computes quantum vacuum expectation values by averaging over a set of suitable weighted random walkers. By means of a procedure called Stochastic Reconfiguration the long standing problem of keeping fixed the walker population without a priori knowledge on the ground state is completely solved. In the  $U(1)_2$  model, which we choose as our theoretical laboratory, we evaluate the mean plaquette and the vacuum energy per plaquette. We find good agreement with previous works using model dependent guiding functions for the random walkers.

PACS numbers: 11.15.Ha, 12.38.Gc

## I. INTRODUCTION

Lattice regularization of quantum field theories is a powerful technique to compute non perturbative physical quantities. Its application to quantum chromodynamics has led to accurate predictions of the spectrum of quark and gluon states as well as of other phenomena like finite temperature phase transitions.

The historical development of this active field of research developed along two main streams: the Lagrangian approach proposed by K. Wilson in 1974 [1] and the Hamiltonian formulation derived by J. Kogut in 1975 [2]. The two approaches are equivalent in the continuum limit but, for the purpose of analytical or numerical investigations, they offer quite different advantages.

The Lagrangian approach exploits Feynman's old idea of computing quantum partition functions as sums over classical histories. Vacuum expectation values are obtained by evaluating suitable statistical averages over long time trajectories. The basic object in this approach is the classical trajectory whose full temporal evolution must be retained. Space and time are treated in a symmetric way and a field configuration is defined over a space time discrete lattice. The identification of a  $d$  dimensional Euclidean quantum theory with a  $d+1$  dimensional statistical model is full. We remark that the Lagrangian approach is the current technique for the study of QCD mass spectra and the most precise studies [3] suggest the advantage of working on anisotropic lattices with different treatment of the spatial and temporal discretisation. In particular, the use of spatially coarse, temporally fine lattices has greatly increased the efficiency of the numerical simulations [4].

These considerations lead to a renewed interest in the Hamiltonian formulation where only space is discretised and time remains continuous. This is a very natural approach in the study of low energy physics. Given the Hamiltonian  $H$  of a quantum many body model, its ground state is projected out by the application of the evolution operator  $U(t) = \exp(-tH)$ , with  $t \rightarrow +\infty$ , to any state with the same quantum numbers of the vacuum. Any accurate representation of the asymptotic behaviour of  $U(t)$  provides access to the ground state and to the low lying excitations. These representations perform clever repeated applications of  $H$ , in analytical or stochastic way, to specific quantum states that replace in this approach the role played by classical trajectories in the Lagrangian one.

One of the first striking examples of this strategy can be found in [5] where the authors obtain good scaling measures of the mass gap in several non trivial models by analytical Lanczos diagonalization of the Hamiltonian. Many other analytical techniques have been developed based on similar ideas like, for instance, resummation of  $U(t)$  expansions or variational approximations to the spectrum. An updated list can be found in [6].

On the numerical side, powerful Monte Carlo algorithms exist for the solution of quantum many body problems [7]. In this paper we are mainly concerned with those belonging to the so called class of Green Function Monte Carlo (GFMC).

They may be regarded as the lattice version of the Feynman-Kac representation [8] for matrix elements of  $U(t)$  that are computed by averaging over ensembles of suitable random walkers. The dynamics of the walkers is determined by the *kinetic* part of the Hamiltonian that is its off diagonal matrix elements in the basis of walker states. The *potential*, the diagonal matrix elements of  $H$ , enters in the definition of a path-dependent weight which the walkers carry to represent their relative importance. In such an approach, the problem

is that the weights exponentially explode or vanish as the walkers diffuse and after a short time the algorithm becomes completely unfeasible.

To solve this problem there are two standard classes of solutions: (a) the introduction of a guiding function for the random walkers, (b) a branching mechanism for the walkers population. Within the former method (see [9–11] for applications to lattice gauge theories), the measure in the path space is deformed and the simulation generates guided random walks according to a guiding function which is inspired by exactly known properties of the ground state (typically, its weak and strong coupling approximations). The disadvantage of the method is that it requires tuning of the functional form of the guiding function. This can only be achieved by a somewhat accurate knowledge of the vacuum structure. In fact, perfect guidance is equivalent to the full problem of determining the vacuum wave function.

In the latter solution, branching is introduced among the walkers to damp their weight variance. Walkers with low weights are deleted and relevant walkers are replicated. The problem in this case is a rather involved management of the variable size walker population.

In a recent paper [12], a simple procedure called Stochastic Reconfiguration, has been successfully applied to overcome this problem and perform simulations with a fixed number of walkers without introducing any guiding function, which can however be exploited if available.

The aim of this paper is to investigate the application of this new technique to lattice gauge theories. In particular, we apply the method to  $U(1)_2$  lattice gauge theory as a simple theoretical laboratory where it is easy to present the main ideas and discuss the systematical errors introduced by the algorithm as well as their control.

The plan of the paper is the following. In Sec. II we review the GFMC with Stochastic Reconfiguration. In Sec. III we apply the algorithm to the  $U(1)_2$  model. We discuss its actual implementation, the optimization of its free parameters and the numerical simulations. Finally, in Sec. IV we summarize our results and discuss the perspectives in the study of realistic gauge models.

## II. REVIEW OF GFMC WITH STOCHASTIC RECONFIGURATION

The description of GFMC with Stochastic Reconfiguration is equivalent to present the Feynman-Kac formula on a lattice. For this reason we begin by discussing the simple example of quantum mechanics in flat space. Let us consider the one dimensional Schrödinger hamiltonian for a unit mass point particle

$$H = \frac{1}{2}p^2 + V(q) = H_0 + V(q) \quad (2.1)$$

and the problem of computing its ground state wave function. We define a discrete Markov chain as follows. Let  $\epsilon$  be the time step (not necessarily infinitesimal) associated to each Markov jump and let the state of the chain be specified by the position eigenvalue  $q$ . Let the transition function  $p(q' \rightarrow q'')$  be

$$p(q' \rightarrow q'') = K_0(q'', q', \epsilon) \quad (2.2)$$

where  $K_0$  is the propagator of the free hamiltonian  $H_0$

$$K_0(q'', q', t) = \langle q'' | \exp -tH_0 | q' \rangle = \frac{1}{\sqrt{2\pi t}} \exp -\frac{(q'' - q')^2}{2t} \quad (2.3)$$

An ensemble of walkers can be described at step  $n$  by its probability density  $P_n(q)$ . It evolves according to

$$P_{n+1}(q'') = \int_{\mathbf{R}} dq' P_n(q') K_0(q'', q', \epsilon) \quad (2.4)$$

We can identify  $P_n(q)$  with the wave function of the abstract state  $|P_n\rangle$  satisfying

$$P_n(q) = \langle q | P_n \rangle \quad (2.5)$$

and therefore, as is well known, we obtain

$$|P_n\rangle = e^{-n\epsilon H_0} |P_0\rangle \quad (2.6)$$

for any finite  $\epsilon$ .

To make a similar construction with  $H_0$  replaced by  $H$  we need an extension of the formalism. We consider a Markov chain where the state is extended from  $q$  to the pair  $(q, \omega)$  where  $\omega$  is a real weight whose dynamics we shall describe in a moment. The transition kernel is assigned as follows

$$p(q'\omega' \rightarrow q''\omega'') = K_0(q'', q', \epsilon) \delta(\omega'' - \omega' e^{-\epsilon V(q')}) \quad (2.7)$$

with the correct normalization

$$\int_{\mathbf{R}} dq'' \int_0^\infty d\omega'' p(q'\omega' \rightarrow q''\omega'') = 1 \quad (2.8)$$

In other words, at each discrete step,  $q$  diffuses making a random step with variance  $\langle (\delta q)^2 \rangle = \epsilon$  as before and the weight  $\omega$  is multiplied by the exponential factor  $\exp(-\epsilon V(q))$ .

The probability distribution  $P_n(q, \omega)$  at the  $n$ -th iteration evolves according to the equation

$$P_{n+1}(q'', \omega'') = \int_{\mathbf{R}} dq' \int_0^\infty d\omega' P_n(q', \omega') p(q', \omega' \rightarrow q'', \omega'') \quad (2.9)$$

To recover a wave function evolving according to  $\exp(-tH)$  we must average over the weights and introduce the function

$$\psi_n(q) = \int_0^\infty d\omega \omega P_n(q, \omega) \quad (2.10)$$

that satisfies

$$\psi_{n+1}(q'') = \int_{\mathbf{R}} dq' \psi_n(q') e^{-\epsilon V(q')} K_0(q'', q', \epsilon) \quad (2.11)$$

If we now write  $\psi_n$  in terms of the associated basis independent abstract state

$$\psi_n(q) = \langle q | \psi_n \rangle \quad (2.12)$$

we easily see that

$$|\psi_{n+1}\rangle = e^{-\epsilon H_0} e^{-\epsilon V(q)} |\psi_n\rangle \quad (2.13)$$

and therefore, by Trotter-Suzuki formula, in the limit  $\epsilon \rightarrow 0$  we obtain

$$\lim_{\epsilon \rightarrow 0} \psi_{t/\epsilon}(q) = \langle q | e^{-tH} | \psi_0 \rangle \quad (2.14)$$

that is the Schrödinger evolution is completely reproduced.

The meaning of the previous manipulations is that we can numerically compute the Schrödinger semigroup by averaging over walkers which diffuse according to the kernel  $K_0$  and which carry an additional weight  $\omega$ . The weight takes care of the potential and is the actual relative weight of the walkers. As discussed in the Introduction, in the actual implementation of this method one has to face the rapidly increasing variance of the weights of an ensemble of walkers as the evolution time goes by.

Stochastic Reconfiguration is a solution to this problem based on the observation that there are many  $P(q, \omega)$  giving rise to the same physical wave function  $\psi(q)$ . In particular

$$\int_0^\infty d\omega \, \omega P(q, \omega) = \int_0^\infty d\omega \, \omega \tilde{P}(q, \omega) \quad (2.15)$$

where

$$\tilde{P}(q, \omega) = \delta(\omega - 1) \int_0^\infty d\omega' \, \omega' P(q, \omega') \quad (2.16)$$

and  $P(q, \omega)$  and  $\tilde{P}(q, \omega)$  give rise to the same wave function  $\psi(q)$ . The difference between them is hidden in the weight statistics that is not observable. The advantage of choosing the representative  $\tilde{P}(q, \omega)$  among all the  $P(q, \omega)$  associated to a given  $\psi(q)$  is that it has exactly zero weight variance by construction since all the weights are fixed to unity.

The actual implementation of Eq. (2.15) in a numerical algorithm is straightforward. Let us consider an ensemble of  $K$  walkers (characterized by their position eigenvalue and weight)

$$\mathcal{E} = \{(q_k, \omega_k)\}_{k=1, \dots, K} \quad (2.17)$$

In the  $K \rightarrow \infty$  limit we can associate to the ensemble  $\mathcal{E}$  a unique well defined distribution function  $P_{\mathcal{E}}(q, \omega)$ . We now build a new ensemble  $\tilde{\mathcal{E}}$  with  $K$  walkers and with the property that when  $K \rightarrow \infty$  we have

$$P_{\tilde{\mathcal{E}}}(q, \omega) = \tilde{P}_{\mathcal{E}}(q, \omega) \quad (2.18)$$

The new ensemble is simply built by extracting walkers from  $\mathcal{E}$  and assigning them a unit weight. The walkers with position  $q_k$  are extracted with probability proportional to  $\omega_k$ . In other words we extract the new  $K$  walkers from the set of old states (the values  $\{q_k\}$ ) with probabilities

$$p_k = \frac{\omega_k}{\sum_k \omega_k} \quad (2.19)$$

Repetitions may occur during this multiple extraction; they change the relative frequency of the old low and high weight walkers. To see this, let us consider an ensemble of walkers

$\{(q_i, \omega_i)\}_{i=1, \dots, K}$  where for simplicity we assume that all  $q_i$  are distinct. We want to compute the statistics of the fractions  $\nu_i = n_i/K$  of walkers with state  $q_i$  in the reconfigured ensemble. Since each new walker is extracted independently, the probability of building a new ensemble with  $n_i$  walkers in the state  $q_i$  is given by the multinomial distribution

$$p(n_1, \dots, n_K) = \frac{K!}{n_1! \dots n_K!} p_1^{n_1} \dots p_K^{n_K} \quad (2.20)$$

The average number of walkers with state  $q_i$  is

$$\langle n_i \rangle = \sum_{n_1 + \dots + n_K = K} \frac{K!}{n_1! \dots n_K!} p_1^{n_1} \dots p_K^{n_K} n_i = K p_i \quad (2.21)$$

and the mean product  $n_i n_j$  with  $i \neq j$

$$\langle n_i n_j \rangle = K(K-1) p_i p_j \quad (2.22)$$

We conclude that

$$\langle \nu_i \rangle = p_i, \quad \langle \nu_i \nu_j \rangle - \langle \nu_i \rangle \langle \nu_j \rangle = -\frac{1}{K} p_i p_j \quad (2.23)$$

Hence, in the reconfigured ensemble the state  $q_i$  appears with a frequency which is precisely  $p_i \sim \omega_i$ . Finite size correlations between the new walkers are present vanishing with  $K$  as  $K^{-1}$ . They induce systematic errors in the measurements that must be eliminated by extrapolation to the limit  $K \rightarrow \infty$ .

We conclude this Section with a comment about Importance Sampling. The aim of this paper is to show that it is possible to perform simulations with a fixed size population of walkers without any a priori knowledge of the vacuum state  $|0\rangle$ . However, it must be emphasized that whenever a trial wave function for  $|0\rangle$  is available, it can be easily included in the algorithm by a unitary transformation of  $H$  as discussed in [13]. This is straightforward in the Hamiltonian formulation and therefore analytical approximations (e.g. variational calculations) can be exploited to accelerate convergence.

### A. Generalization to other models

From the above discussion, it should be clear that the extension of GFMC with Stochastic Reconfiguration to a more general Hamiltonian is possible only when some structural conditions are true. To be definite we require the existence of a complete explicit basis  $\{|s\rangle\}$  such that  $H$  can be written

$$H = T + V \quad (2.24)$$

where: (a)  $V$  is real and has vanishing off diagonal matrix elements, (b)  $T$  is the generator of a Markov process. Condition (b) is simply the statement that the evolution operator  $U(t) = \exp(-t T)$  exists for  $t > 0$  and the kernel

$$K(s'', s', t) = \langle s'' | \exp(-t T) | s' \rangle \quad (2.25)$$

is positive and normalized

$$\sum_{s''} K(s'', s', t) = 1 \quad (2.26)$$

In more physical terms, we require to be able to write the Hamiltonian as a potential term plus a *good* kinetic term like, on a generic manifold, the Laplace-Beltrami operator which is associated to random walks on the manifold. Interesting models which belong to this class in the Hamiltonian formulation are the non linear  $O(N)$   $\sigma$  model and the  $SU(N)$  pure gauge theories.

## B. Observables Measurements

In this Section we discuss how observables can be measured. The ground state energy is the simplest observable to be computed. To measure it, we take two arbitrary states  $|\chi\rangle$  and  $|\psi\rangle$  with non zero overlap with the ground state  $|0\rangle$  and write

$$E_0 = \lim_{t \rightarrow +\infty} \frac{\langle \chi | H e^{-tH} | \psi \rangle}{\langle \chi | e^{-tH} | \psi \rangle} \quad (2.27)$$

The state  $|\psi\rangle$  describes the statistics of the initial state of the chain. A convenient choice, although not always optimal, is to take for  $|\psi\rangle$  one of the walker states and to start accordingly the Markov chain always from the same state. About  $|\chi\rangle$ , a good choice is to take the zero momentum state which is annihilated by the kinetic (off-diagonal) part of  $H$ . In other word, this is the generalization (on non flat manifold) of the constant wave function. In this case we drop the kinetic part of  $H$  and obtain

$$E_0 = \lim_{t \rightarrow +\infty} \frac{\langle \chi | V e^{-tH} | \psi \rangle}{\langle \chi | e^{-tH} | \psi \rangle} \quad (2.28)$$

where  $V$  is the diagonal part of  $H$ . From the point of view of the algorithm, the projection over  $|\chi\rangle$  is nothing but the recipe of summing over all the walkers with no additional final state weight.

These prescriptions may be refined in model dependent ways, but we shall see that, at least in the model under consideration, they work properly.

Concerning other operators, let us analyze in some details the measure of vacuum expectation values of operators  $Q$  which are diagonal in the chosen basis (the position eigenstates in the Schrödinger example). They can be computed as the limit

$$\frac{\langle 0 | Q | 0 \rangle}{\langle 0 | 0 \rangle} = \lim_{\tau \rightarrow +\infty} \mathcal{O}(\tau) \quad (2.29)$$

where

$$Q(\tau) = \lim_{t \rightarrow +\infty} \frac{\langle \chi | e^{-\tau H} Q e^{-tH} | \psi \rangle}{\langle \chi | e^{-(\tau+t)H} | \psi \rangle} = \langle 0 | Q | 0 \rangle + \mathcal{O}(e^{-\tau(E_1 - E_0)}) \quad (2.30)$$

where  $E_1$  is the energy of the first excited state  $|1\rangle$  with non vanishing matrix element  $\langle 1 | Q | 0 \rangle$ . In the above expression, the limit over  $t$  is performed automatically by the running

of the Markov chain. It can be considered reached as soon as equilibrium in the chain is achieved. The second limit requires some care and to evaluate it we allow the walkers to diffuse for an additional time  $\tau$  after the measurement of the observable. In the following Sections we shall check the rapid exponential convergence of  $Q(\tau)$  with increasing  $\tau$ . Of course, from the  $\tau$  dependence of  $Q(\tau)$  the (finite volume) mass gap  $E_1 - E_0$  can be extracted.

### III. APPLICATION TO THE $U(1)_2$ MODEL

In this Section we make the previous discussion more detailed by examining a specific example, the  $U(1)_2$  lattice gauge model. Its Hamiltonian is given by

$$H = \sum_{p=1}^L \left[ \left( \sum_{l_p=1}^3 -\frac{1}{2\beta} \frac{\partial^2}{\partial \theta_{l_p}^2} \right) + \beta(1 - \cos \phi_p) \right] \quad (3.1)$$

where the link phases  $\theta_{l_i}$  are defined in Fig. 1 and the gauge invariant plaquette phase  $\phi_p$  is

$$\phi_p = \theta_{1,p} + \theta_{2,p+1} - \theta_{3,p} - \theta_{2,p} \quad (3.2)$$

We assume periodic boundary conditions. This lattice model has no continuum limit because its correlation length in lattice units remains finite for all values of the coupling  $\beta$ . Nonetheless, it shares many features with the more realistic models in higher dimensions and serves to illustrate the method in an easy case. We are interested in the numerical calculation of the ground state energy per plaquette  $E_0/N$  and of the mean plaquette

$$\langle U_p \rangle \equiv \langle 0 | \cos \phi_p | 0 \rangle \quad (3.3)$$

For these two observables, the first terms in the weak and strong coupling expansions are known [10]

$$\frac{E_0}{L} = \begin{cases} \beta - \frac{1}{4}\beta^3 + \frac{89}{3840}\beta^7 + \mathcal{O}(\beta^{11}) \\ 0.9833 - 0.1209\beta^{-1} + \mathcal{O}(\beta^{-2}) \end{cases} \quad (N \geq 5) \quad (3.4)$$

$$\langle U \rangle = \begin{cases} \frac{1}{2}\beta^2 - \frac{89}{960}\beta^6 + \mathcal{O}(\beta^{10}) \\ 1 - 0.4917\beta^{-1} + \mathcal{O}(\beta^{-2}) \end{cases} \quad (3.5)$$

#### A. Optimization of the Algorithm

Let us discuss in this Section the tuning of the algorithm. Its free parameters are

$$\epsilon, \quad K, \quad r, \quad \tau \quad (3.6)$$

where  $\epsilon$  is the time step in the application of  $\exp(-\epsilon H)$ ,  $K$  is the size of the walkers ensemble,  $r$  is the number of Markov chain steps between two reconfigurations and  $\tau$  is the time which



we discussed in Sec. II B. The best choice of  $\tau$  of course depends on the chosen observable. In principle, the same holds also for the first three parameters, but for simplicity, we shall discuss their optimization on general grounds independently on  $Q$ .

The parameter  $\epsilon$  sets the scale of the elementary fluctuations of the link phases  $\theta$ . Since  $\langle(\delta\theta)^2\rangle = \epsilon$  we require  $\sqrt{\epsilon} \sim 2\pi/n_\theta$  with large  $n_\theta$  to obtain a good approximation of the continuum diffusion. In our simulations we choose the conservative value  $n_\theta = 50$  and therefore  $\epsilon = 0.015$ .

The value of  $K$  cannot be fixed. Instead, it must be varied and an extrapolation to  $K = \infty$  is needed. The following functional form for all  $K$  dependent quantities

$$Q(K) = Q(\infty) + \frac{c}{K^\alpha} + \dots \quad (3.7)$$

turns out to be enough general to reproduce quite well the  $K$  dependence. In our simulation we extract the three constants  $Q(\infty)$ ,  $c$  and  $\alpha$  from  $Q(K)$  at  $K = 10, 100, 1000, 5000$ .

The parameter  $r$  controls the frequency of the reconfiguration process. A small  $r$  is useless and expensive. Actually, reconfiguration must be performed only when the walkers begin to show a significantly large weight variance. In that case, reconfiguration is effective. If the variance is small, then reconfiguration reshuffles the ensemble without useful effects. On the other hand, if  $r$  is taken too large, reconfiguration with a finite  $K$  will destroy the information contained in the ensemble and the systematic error at fixed  $K$  will be large. Our proposal for a choice of an optimal  $r$  is to fix it by looking at the integrated autocorrelation time of a relevant observable, say the vacuum energy. We set  $r = 1$  and run the algorithm: the energy measurements  $\{E_i\}$  show an exponential decorrelation

$$\overline{E_n E_m} - \overline{E}^2 \sim A e^{-|n-m|/\tau} \quad (3.8)$$

where as usual bars denote the average over the measurements. We then set  $r \equiv \tau$ . This procedure has two advantages: (a) the energy measurements taken after each reconfiguration are decorrelated, (b) the autocorrelation  $\tau$  is independent on  $K$ . Statement (a) holds by construction. Property (b) follows from the fact that  $\tau$  is an intrinsic feature of the chaotic evolution of each single walker and has no reason to be  $K$  dependent as we have checked explicitly. This is a useful property for the  $K \rightarrow \infty$  extrapolation.

In our simulations we consider the  $U(1)_2$  model at  $\beta = 0.5, 1.0, 1.5, 2.0, 2.5$  with  $L = 8$  to reproduce the results of [10]. In this case we find that the optimal  $r(\beta)$  is roughly

$$r(0.5) = 40, \quad r(1.0) = 30, \quad r(1.5) = 25, \quad r(2.0) = 25, \quad r(2.5) = 20 \quad (3.9)$$

We now present our results for the ground state energy per plaquette and mean plaquette. For each data point we performed  $10^5$  Markov chain steps.

## B. Measure of $E_0$

We have computed the vacuum energy per plaquette at the four values  $K = 10, 100, 1000$  and 5000 on a  $L = 8$  spatial lattice. A fit with the functional form in Eq. (3.7) determines the  $\beta$  dependent exponent  $\alpha(\beta)$ . In Fig. (2) we show the linear fit of the numerical measures plotted as functions of  $1/K^{\alpha(\beta)}$ . The results of the fit are collected in Tab. (I) and compared

with the weak and strong coupling expansions. The results are quite good, especially because the strong coupling series is only known up to the next to leading term. The CPU time required for each point is about one hour on a Pentium 200 processor. Moreover, we stress that to obtain these results we only needed a very simple tuning of the algorithm and no additional knowledge of the ground state properties. As can be seen from the figure, the extrapolation is very near the value obtained with the largest  $K$  used. In the present model, it is fairly easy to obtain analytical approximations for the ground state energy per plaquette. The hamiltonian written in terms of the gauge invariant phases  $\phi_p$  is

$$H = \sum_{p=1}^N \left[ \frac{1}{\beta} \left( -2 \frac{\partial^2}{\partial \phi_p^2} + \frac{\partial^2}{\partial \phi_p \partial \phi_{p+1}} \right) + \beta(1 - \cos \phi_p) \right], \quad (3.10)$$

and the independent plaquette approximation gives

$$\frac{E_0^{(Mathieu)}}{L} = \beta + \frac{1}{2\beta} a_0(-\beta^2), \quad (3.11)$$

where  $a_0(q)$  is the lowest characteristic value for the even solutions of the Mathieu equation

$$y''(x) + (a_0(q) - 2q \cos(2x))y = 0. \quad (3.12)$$

A more practical approximation can be obtained by a variational calculation based on the following simple independent plaquette Ansatz

$$\psi_0(\phi_1, \dots, \phi_N) = \exp \left( \lambda \sum_{p=1}^N \cos \phi_p \right). \quad (3.13)$$

In this case we obtain

$$\frac{E_0^{(var)}(\beta)}{L} = \beta + \frac{1}{\beta} \min_{\lambda} \left[ (\lambda - \beta^2) \frac{I_1(2\lambda)}{I_0(2\lambda)} \right], \quad (3.14)$$

(where  $I_n$  is the n-th modified Bessel function). In Tab. (I), columns *Mathieu* and *var* show the numerical values of these approximations.

As one can see, they appear to reproduce well the Monte Carlo data over the whole region of the coupling. This holds true especially for the estimate computed in terms of Mathieu functions. However, we stress again that the Monte Carlo extrapolated data have no systematic errors and have been obtained with the minimum a priori knowledge. As stated above, any analytical information on the ground state, like a variational ground state wave function, can be used for the acceleration of the Monte Carlo simulation by including in the algorithm an importance sampling step.

### C. Measure of $\langle U_p \rangle$

The results obtained for the average plaquette are quite similar to the previous ones. Again, we show in Fig. (3) the linear extrapolation after the determination of  $\alpha(\beta)$ . In Tab. (II) we see that the Monte Carlo data is well matching the analytical series except

in the region around  $\beta = 1.0$ . However, the weak coupling series is not to be trusted at  $\beta = 1.0$  since its plot shows a steep variation between  $\beta = 1.0$  and  $\beta = 1.5$  signalling the need for an additional term. The point at  $\beta = 1.5$  deviated by about 3% with respect to the strong coupling series. This can simply explained by assuming that it is a too small value for strong coupling to apply and moreover the next points at larger  $\beta$  match better, below the percent level. In Fig. (4) we show the dependence of  $\langle U(\tau) \rangle$  on the time  $\tau$  to check the exponential convergence to the vacuum expectation value. Again, we stress that these numbers are obtained without a priori information and over the whole coupling variation.

To summarize our results we collect in Fig. (5) a graphical comparison of Monte Carlo data with the asymptotic  $\beta \rightarrow 0$  and  $\beta \rightarrow \infty$  expansions.

#### D. Computational Cost

In this Section we address the problem of estimating the computational cost of the algorithm. A realistic computation must follow two steps:

- a) extrapolation  $K \rightarrow \infty$  at fixed coupling  $\beta$ :
- b) continuum limit  $\xi(\beta) \rightarrow \infty$  where  $\xi$  is the correlation length in lattice units (we do not discuss finite volume effects and their control).

In performing step (a) we need the computational cost as a function of  $K$  that is the CPU time required to achieve a give statistical error  $\epsilon_{stat}$  in the evaluation of an observable  $Q$ . With  $N$  Markov chain steps we have

$$\epsilon_{stat} = \frac{\sigma(\beta, K)}{\sqrt{N/r(\beta)}} \quad (3.15)$$

where  $\sigma_Q(\beta, K)$  is the standard deviation of  $Q$  measurements and  $N/r(\beta)$  is the number of independent measurements. The dependence of  $\sigma_Q$  on  $K$  is simple. Due to a self average effect we expect  $\sigma_Q(\beta, K) = \tilde{\sigma}_Q(\beta)K^{-1/2}$ . Our explicit numerical simulations confirm this scaling law. The CPU time is roughly proportional to  $NK$  since the reconfiguration process turns out to be only a small fraction of the computational cost. Therefore

$$\epsilon_{stat} \sim \frac{\tilde{\sigma}(\beta)}{\sqrt{T_{CPU}/r(\beta)}} \quad (3.16)$$

and  $K$  cancels. The increase in CPU time associated to the management of the ensemble is compensated by the larger statistics. In other words, the cost of stochastic reconfiguration is just the cost of the fit described by Eq. (3.7): it is proportional to  $p$  the number of  $k$  values used to extract  $Q(\infty)$  from  $Q(K)$ .

The cost of step (b) is expected to be much more model dependent. As the continuum limit is approached, the quantities which vary with  $\beta$  are  $\tilde{\sigma}(\beta)$ ,  $r(\beta)$  and  $\alpha(\beta)$ . There is no mechanism in this algorithm to prevent slowing due to increasing  $r(\beta)$  when the correlation length increases and the behaviour of the algorithm must be studied in the case of realistic models with diverging correlation length. What we observe in the considered model is a

very mild  $\beta$  dependence of the exponent  $\alpha(\beta)$  suggesting that Eq. (3.7) may hold without the need for a huge  $K$ . Moreover, an advantage of the Hamiltonian formulation is that this slowing could be eventually reduced by importance sampling as discussed in the end of Sec. II; in fact, preliminary investigations show that the use of a good trial wave function for the ground state can strongly reduce  $\tilde{\sigma}_Q(\beta)$  and allow to perform simulations with reasonable errors using relatively small values of  $K$ .

#### IV. CONCLUSIONS AND PERSPECTIVES

In this paper we applied a recently proposed many body Monte Carlo algorithm of Green Function type to the study of lattice gauge models in Hamiltonian form. This kind of algorithms compute the vacuum wave function and many related quantities by averaging over a set of suitable weighted random walkers. The method that we discussed solves the annoying long standing problem of fixing the walkers number without exploiting a priori informations on the ground state structure and is thus quite general. The trade off is the introduction of a systematic error, but we showed by explicit simulations in the  $U(1)_2$  model that it can be kept completely under control. The algorithm can be applied to more interesting models like the non linear  $O(N)$   $\sigma$  model or  $SU(N)$  pure gauge on which work is in progress [14]. The perspectives of this works seem interesting especially in view of the recently proposed improved lattice Hamiltonians [15] for pure gauge models where we plan to investigate the algorithm efficiency.

#### ACKNOWLEDGMENTS

I thank Prof. G. Jona-Lasinio for many discussions on the Feynman-Kac formula and its related quantum many body algorithms. I also thank Prof. G. Curci for many useful discussions on the numerical simulation of lattice field theories. Finally, financial support from INFN Iniziativa Specifica RM42 is acknowledged.

## REFERENCES

- [1] K. Wilson , Phys. Rev. D **10** , 2445 (1974).
- [2] J. B. Kogut and L. I. Susskind , Phys. Rev. D **11** , 395 (1975); J. B. Kogut , Rev. Mod. Phys. **51** , 659 (1979).
- [3] C. J. Morningstar and M. Peardon , Phys. Rev. D **60** , 034509 (1999)
- [4] C. J. Morningstar and M. Peardon , Phys. Rev. D **56** , 4043 (1997).
- [5] A. Duncan and R. Roskies , Phys. Rev. D **31** , 364 (1985); A. Duncan and R. Roskies , Phys. Rev. D **32** , 3277 (1985); J. W. Choe, A. Duncan and R. Roskies , Phys. Rev. D **37** , 472 (1988).
- [6] S. H. Guo and X. Q. Luo, Los Alamos Preprint hep-lat/9706017.
- [7] W. von der Linden , Phys. Rep. **220** , 53 (1992).
- [8] B. Simon, “Functional integration and quantum physics”, Academic Press, Inc., New York (1979).
- [9] S. A. Chin, O. S. van Roosmalen, E. A. Umland and S. E. Koonin , Phys. Rev. D **31** , 3201 (1985); S. A. Chin, C. Long and D. Robson , Phys. Rev. D **37** , 3001 (1988); C. Long, D. Robson and S. A. Chin , Phys. Rev. D **37** , 3006 (1988).
- [10] T. Barnes and D. Kotchan , Phys. Rev. D **35** , 1947 (1987).
- [11] C. J. Hamer, K. C. Wang and P. F. Price , Phys. Rev. D **50** , 4693 (1994); C. J. Hamer, R. J. Bursill and M. Samaras, “Green’s Function Monte Carlo Study of Correlation Functions in the  $(2 + 1)D$   $U(1)$  lattice gauge theory”, hep-lat/0002001.
- [12] M. C. Buonaura and S. Sorella , Phys. Rev. B **57** , 11446 (1998); J. A. Hetherington , Phys. Rev. A **30** , 2713 (1984).
- [13] D. M. Ceperley and M. H. Kalos in “Monte Carlo Methods in Statistical Physics”, ed. K. Binder, Springer-Verlag, Heidelberg (1992).
- [14] M. Beccaria and A. Moro, in preparation.
- [15] X. G. Luo, S. H. Guo, H. Kröger and D. S. Schütte , Phys. Rev. D **59** , 034503 (1999).

## FIGURES

FIG. 1.  $U(1)$  N-chain geometry. Definition of the link angles.

FIG. 2. Extrapolation  $K \rightarrow \infty$  for the vacuum energy per plaquette.

FIG. 3. Extrapolation  $K \rightarrow \infty$  for the mean plaquette.

FIG. 4. Large  $\tau$  limit of  $\langle U(\tau) \rangle$ .

FIG. 5. Graphical comparison of Monte Carlo data with strong and weak coupling series.

# TABLES

TABLE I.  $E_0/L$  compared with weak and strong coupling approximations. The last column shows the relative deviation between the Monte Carlo (MC) data and the weak or strong expansions.

$\beta$	weak	MC	Mathieu	var	strong	% $\Delta$
0.5	0.4689	0.4694(2)	0.4690	0.4690	—	0.1
1.0	0.7732	0.7736(2)	0.7724	0.7746	—	0.05
1.5	—	0.8907(2)	0.8909	0.9005	0.9027	1
2.0	—	0.9292(2)	0.9299	0.9435	0.9229	0.7
2.5	—	0.9524(2)	0.9466	0.9594	0.9349	2

TABLE II.  $\langle U \rangle$  compared with weak and strong coupling approximations.

$\beta$	weak	MC	strong	% $\Delta$
0.5	0.1236	0.1229(2)	—	0.6
1.0	0.4073	0.4262(2)	—	5
1.5	—	0.6513(2)	0.6722	3
2.0	—	0.7590(2)	0.7542	0.6
2.5	—	0.8074(2)	0.8033	0.5

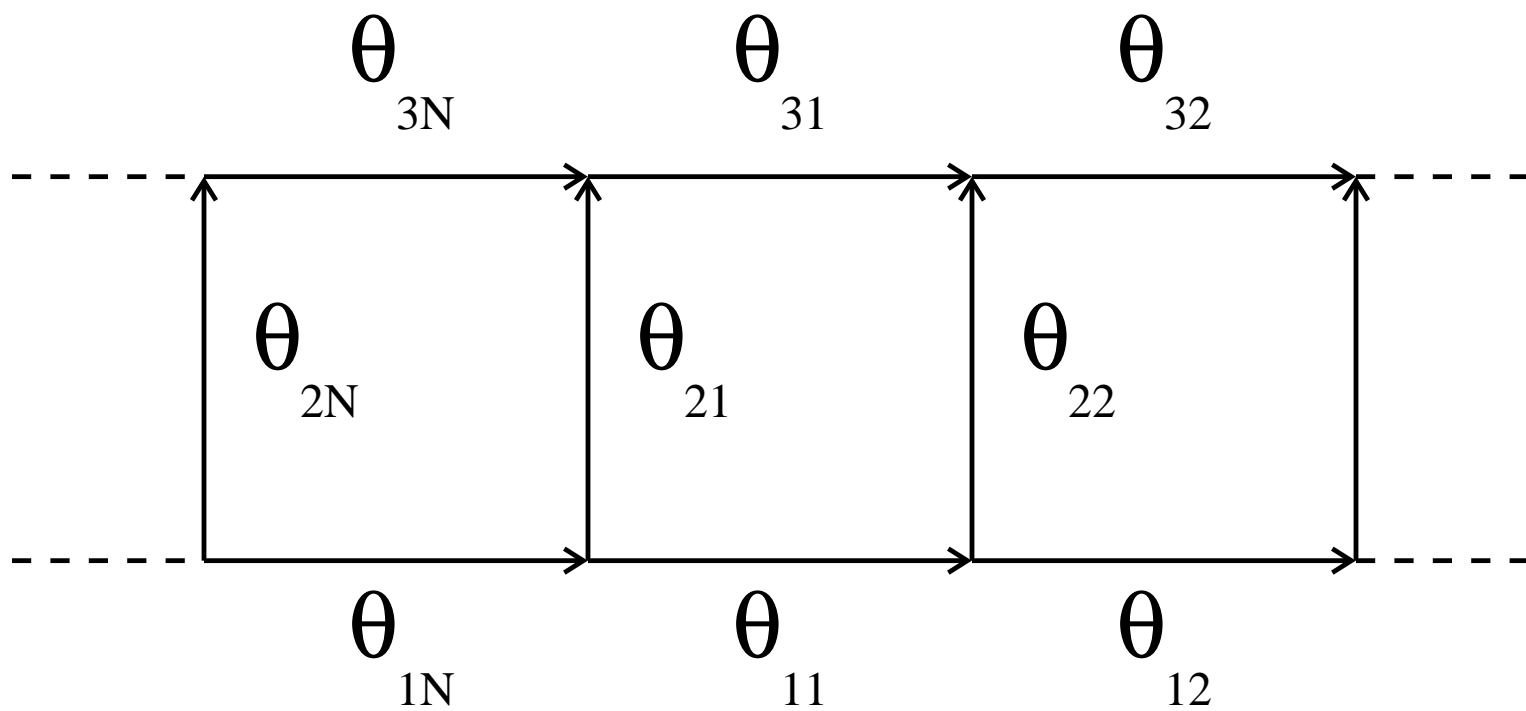


Figure 1



Figure 2

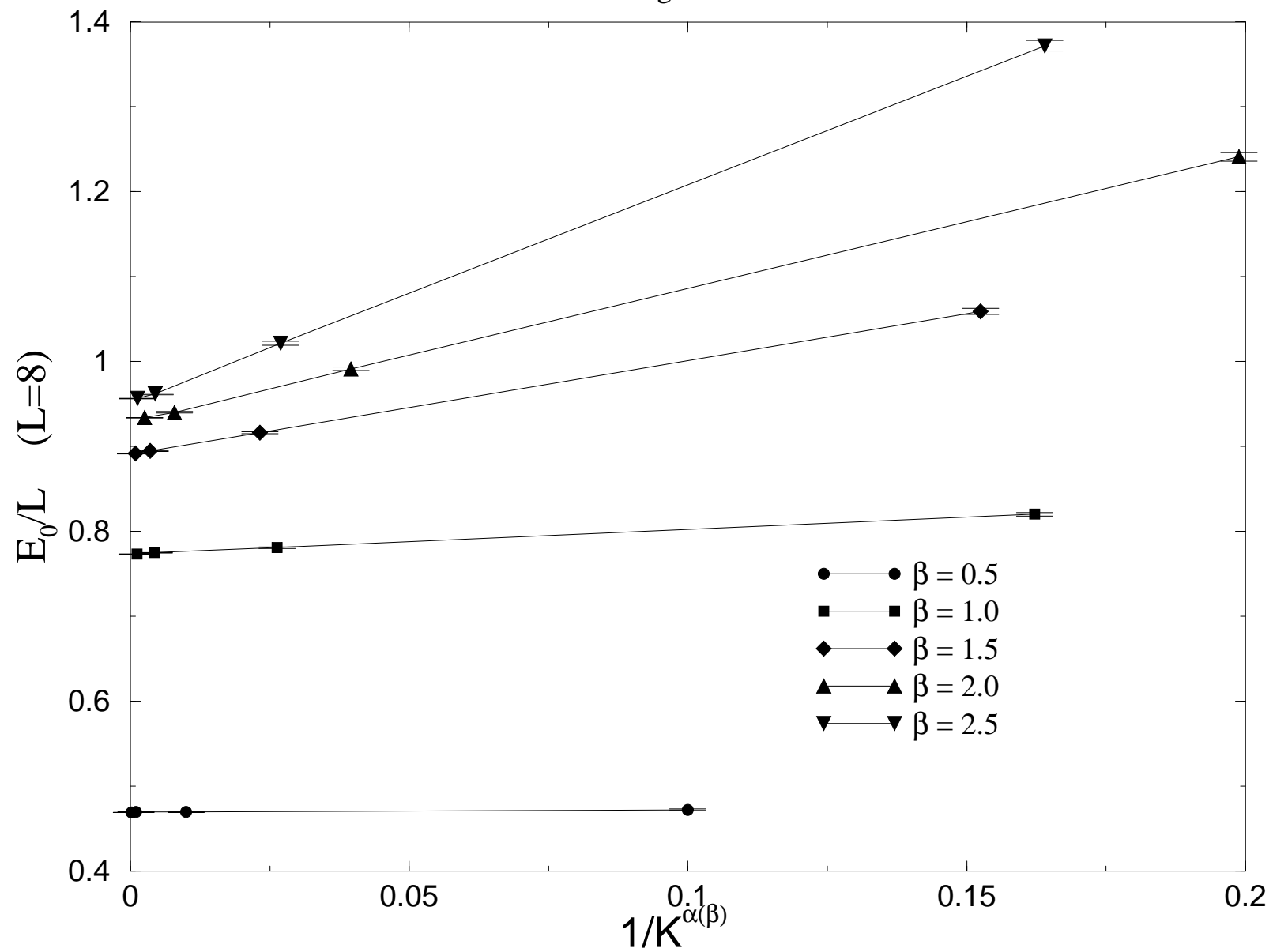


Figure 3

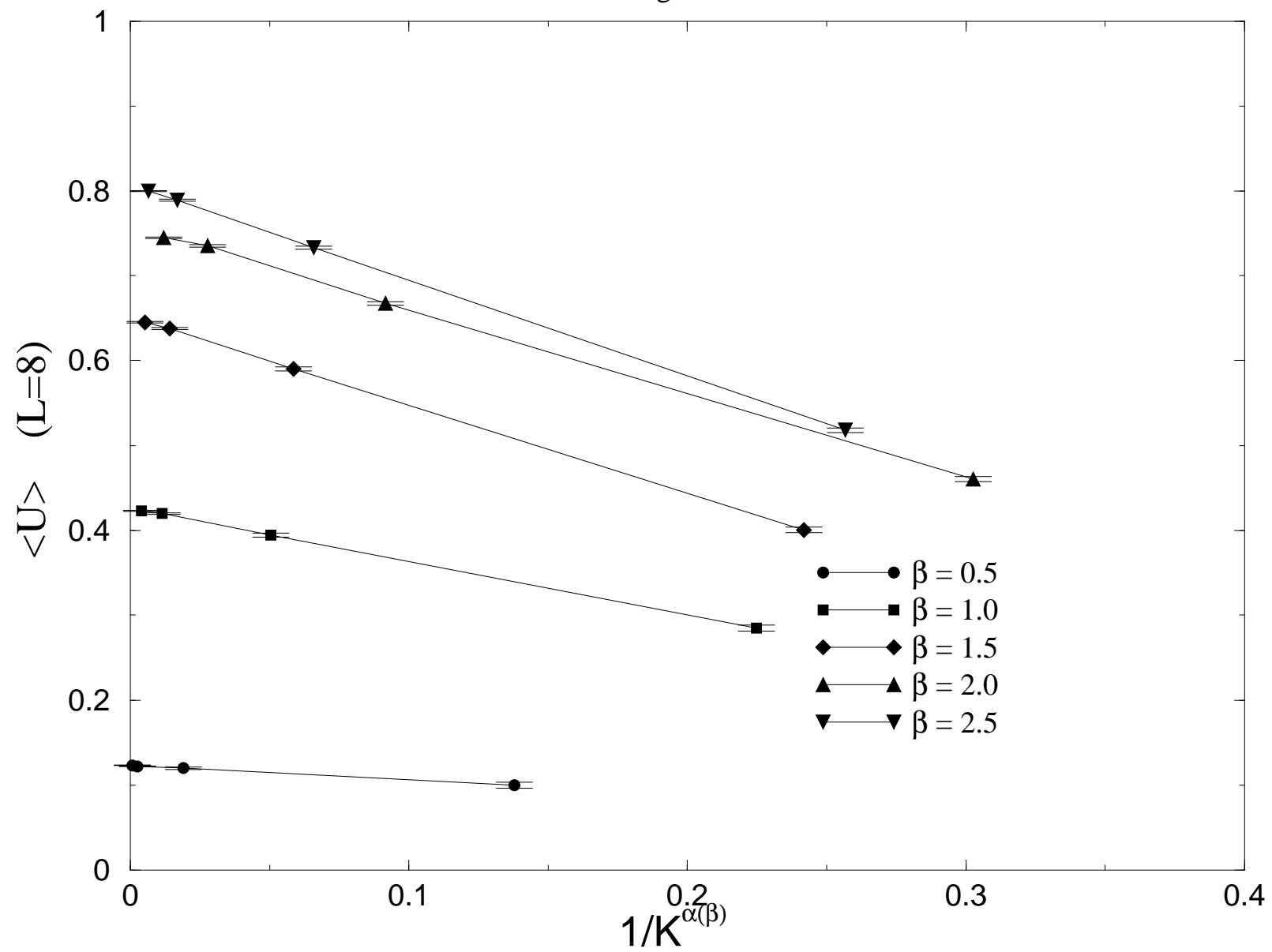


Figure 4

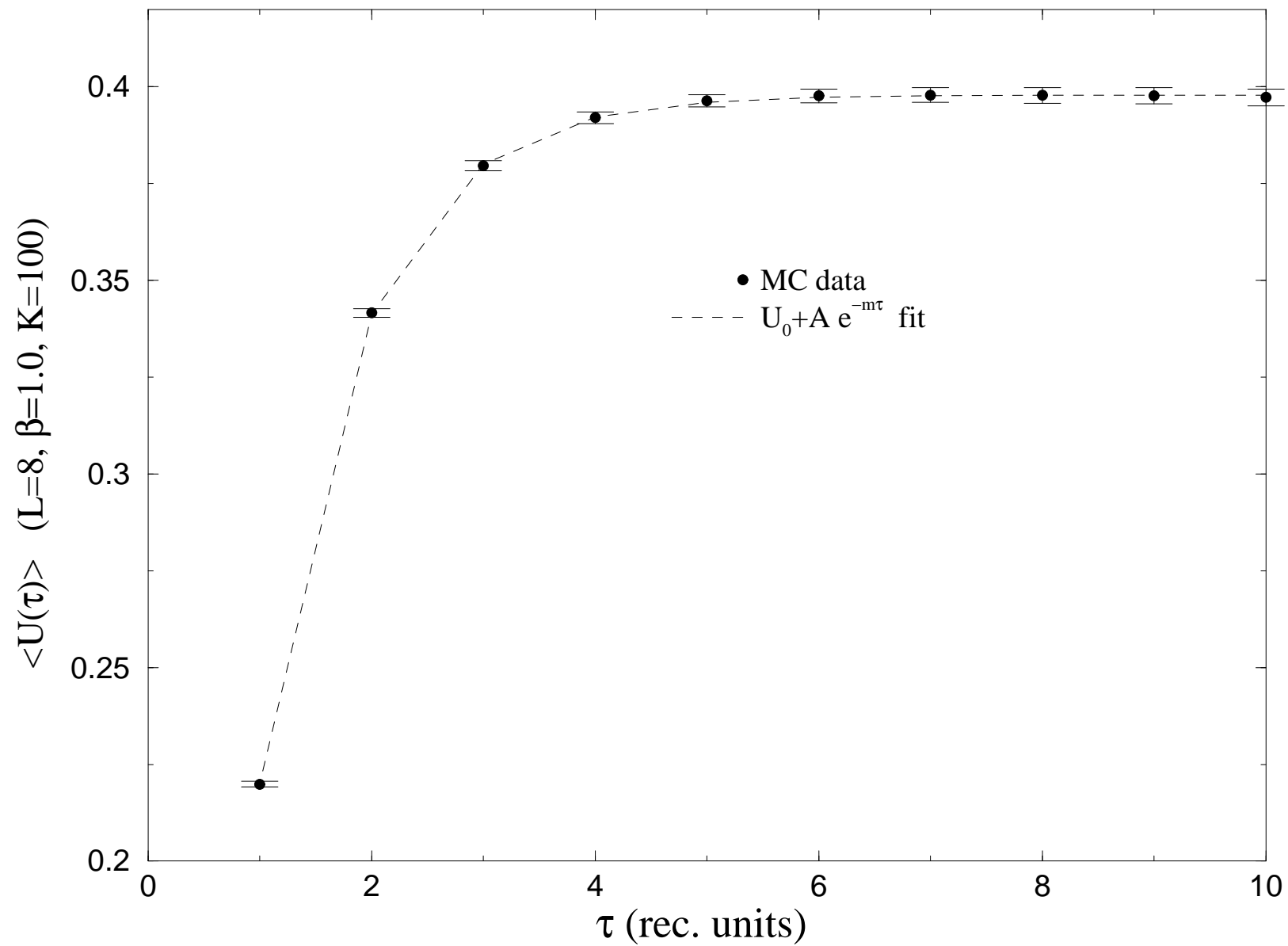


Figure 5

